REFERENCES AND NOTES

1. There is a subclass of NIDDM referred to as maturity-onset diabetes of the young (MODY). This probably has an etiology distinct from that of most NIDDM (possibly involving an abnormality in the glucokinase gene) [N. Vionnet *et al.*, *Nature* **356**, 721 (1992)].
2. R. H. Unger and L. Orci, in *Handbook of Experimental Pharmacology: Glucagon II*, P. J. Lefèbvre, Ed. (Springer-Verlag, Berlin, 1983), pp. 431–450; J. D. McGarry, K. F. Woeltje, M. Kuwajima, D. W. Foster, *Diabetes Metab. Rev.* **5**, 271 (1989).
3. J. D. McGarry, *Diabetes* **28**, 517 (1979); _____ and D. W. Foster, *Annu. Rev. Biochem.* **49**, 395 (1980).
4. Randle proposed that a reciprocal relation exists between glucose and fatty acid oxidation. If fatty acid oxidation is operative, glucose uptake and oxidation would be impaired [P. J. Randle, A. L. Kerbey, J. Espinal, *Diabetes Metab. Rev.* **4**, 623 (1988)].
5. J. D. McGarry and D. W. Foster, *J. Clin. Invest.* **52**, 877 (1973).
6. C. J. Bailey and P. R. Flatt, in *New Antidiabetic Drugs*, C. J. Bailey and P. R. Flatt, Eds. (Eldred Smith-Gordon, London, 1990), pp. 231–236, H. P. O. Wolf, *ibid.*, pp. 217–229.
7. E. O. Balasse and M. A. Neef, *Eur J. Clin. Invest.* **4**, 247 (1974); *Metab. Clin. Exp.* **22**, 1193 (1973).
8. R. A. De Fronzo, R. C. Bonadonna, E. Ferrannini, *Diabetes Care* **15**, 318 (1992).
9. In this procedure, insulin and glucose are infused to achieve the desired level of hyperinsulinemia while maintaining euglycemia. Ordinarily, this results in the cessation of hepatic glucose output such that the rate of glucose infusion equals its rate of disposal.
10. G. M. Reaven, C. Hollenbeck, C.-Y. Jeng, M. S. Wu, Y.-D. I. Chen, *Diabetes* **37**, 1020 (1988).
11. Y.-D. I. Chen, A. Golay, A. L. M. Swislocki, G. M. Reaven, *J. Clin. Endocrinol. Metab.* **64**, 17 (1987).
12. G. M. Reaven, H. Chang, B. B. Hoffman, *Diabetes* **37**, 28 (1988).
13. C. Saloranta, A. Franssila-Kallunki, A. Ekstrand, M.-R. Taskinen, L. Groop, *Diabetologia* **34**, 409 (1991).
14. K. Ratheiser *et al.*, *Metabolism* **40**, 1185 (1991).
15. A. Vaag, J. E. Henriksen, H. Beck-Nielsen, *J. Clin. Invest.* **89**, 782 (1992).
16. It is assumed that differences in circulating insulin concentrations primarily reflect changes in hormone secretion rather than alterations in the rate of clearance.
17. M. D. Schumacher, S. J. Hasstedt, S. C. Hunt, R. R. Williams, S. C. Elberin, *Diabetes* **41**, 416 (1992).
18. A. E. Pontiroli, M. Alberetto, G. Pozza, *Diabetologia* **35**, 294 (1992).
19. N. Zarjevski, P. Doyle, B. Jeanrenaud, *Endocrinology* **130**, 1564 (1992).
20. S. L. Marban, *Diabetes* **41**, 145A (abstr. 516) (1992).
21. K. Falholt *et al.*, *Diabet. Med.* **540**, 27 (1988).
22. L. H. Storlien *et al.*, *Diabetes* **40**, 280 (1991).
23. A. A. Young, L. B. Crocker, D. Wolfe-Lopez, G. J. S. Cooper, *FEBS Lett.* **287**, 203 (1987).
24. D. Wititsuwannakul and K. H. Kim, *J. Biol. Chem.* **252**, 7812 (1977).
25. R. H. Unger, *Science* **251**, 1200 (1991).
26. Cited work from the author's laboratory was supported by grants from NIH (DK18573 and DK11313) and the Juvenile Diabetes Foundation.

RESEARCH ARTICLE

Femtosecond Resolution of Soft Mode Dynamics in Structural Phase Transitions

Thomas P. Dougherty, Gary P. Wiederrecht, Keith A. Nelson,
Mark H. Garrett, Hans P. Jensen, Cardinal Warde

The microscopic pathway along which ions or molecules in a crystal move during a structural phase transition can often be described in terms of a collective vibrational mode of the lattice. In many cases, this mode, called a "soft" phonon mode because of its characteristically low frequency near the phase transition temperature, is difficult to characterize through conventional frequency-domain spectroscopies such as light or neutron scattering. A femtosecond time-domain analog of light-scattering spectroscopy called impulsive stimulated Raman scattering (ISRS) has been used to examine the soft modes of two perovskite ferroelectric crystals. The low-frequency lattice dynamics of KNbO$_3$ and BaTiO$_3$ are clarified in a manner that permits critical evaluation of microscopic models for their ferroelectric transitions. The results illustrate the advantages of ISRS over conventional Raman spectroscopy of low-frequency, heavily damped soft modes.

The manner in which cooperative structural change occurs in condensed matter has been examined extensively. Structural phase transitions between different crystalline forms are particularly amenable to study because the microscopic pathway along which ions or molecules in the lattice move from their positions in one phase to their positions in the other may be inferred from x-ray and other spectroscopic analysis of the two phases. This microscopic pathway may be considered a cooperative "reaction coordinate" for the phase transition, which in some respects may be thought of as a cooperative chemical reaction. Unimolecular chemical reaction coordinates are described in terms of molecular vibrational modes, or tunneling (or thermally assisted hopping) between different local potential energy minima, or both; cooperative motions in structural phase transitions are described in terms of lattice vibrational modes or hopping degrees of freedom. In both cases, a microscopic understanding requires information about the potential energy surface along which "reaction" occurs and about the dynamics of motion along this surface. In the molecular case, both time-domain and frequency-domain experimental methods have been used extensively (*1*). Time-resolved spectroscopy has been possible because optical absorption provides a mechanism with which to initiate motion along excited-state photochemical reaction coordinates. In the collective case, frequency-domain spectroscopic methods have been used almost exclusively (*2*), mainly because phase transitions occur in ground electronic states and a mechanism for controlled optical initiation of the microscopic motions involved in phase transitions has not been available.

Structural phase transitions can be described in two limiting cases as either displacive or order-disorder, and are characterized, respectively, by a single potential energy minimum whose position shifts at the transition temperature T_c or by several minima among which a "choice" is made at T_c (*3*) (Fig. 1). For displacive transitions, motion between the two phases involves lattice vibrations that are termed "soft" modes because of their reduced frequencies near T_c (*4, 5*). Order-disorder transitions occur through collective tunneling or thermally assisted hopping modes. Lattice vibrational and hopping modes are usually examined through Raman spectroscopy (*2*), in which their signatures may be very different. Most lattice vibrations show distinct Stokes and anti-Stokes Raman features whose frequency shifts and widths yield quantitative values of the vibrational frequency and dephasing rate, whereas hopping modes give rise to central peaks whose widths yield the hopping rates. Unfortunately, soft vibrational modes generally show low frequencies and very strong damping near T_c so that the Stokes and anti-Stokes lines merge into a broad central peak that closely resembles

---

T. P. Dougherty, G. P. Wiederrecht, and K. A. Nelson are in the Department of Chemistry, M. H. Garrett and H. P. Jenssen are in Center for Materials Science and Engineering, and C. Warde is in the Department of Electrical Engineering and Computer Science at the Massachusetts Institute of Technology, Cambridge, MA 02139.

the peak that is characteristic of hopping modes. In addition, most phase transitions show both displacive and order-disorder character. Both heavily damped vibrational and relaxational (that is, hopping) modes may contribute to low-frequency Raman spectra, and it is often impossible to analyze the spectra uniquely. Because of the lack of information about the dynamics of cooperative motion, a quantitative microscopic description is available for very few structural phase transitions.

We report femtosecond time-resolved observations of heavily damped soft modes involved in structural phase transitions. The excitation mechanism for initiation of the cooperative motion is impulsive stimulated Raman scattering (ISRS) (*6–8*). In ISRS, ultrashort excitation pulses exert a sudden ("impulsive") driving force on Raman-active modes whose time-dependent responses are monitored through coherent scattering of variably delayed probe pulses. Time-domain observation through impulsive stimulated scattering offers distinct advantages for characterization of heavily damped modes and for distinguishing their responses from those of other low-frequency excitations. This method has been used in liquids where heavily damped intermolecular vibrations (*9*) and shear acoustic waves (*10*) have been observed. In crystals, soft acoustic phonons have been characterized (*11*). ISRS observations of optic phonons (*6, 12, 13*) have so far been restricted to lightly damped modes that could also be characterized well through Raman spectroscopy. The current experiments were done on modes whose study through Raman spectroscopy has produced widely varying results (*14–19*). We note that ISRS experiments are very different from femtosecond heating experiments in which melting (and even vaporization) is induced but little detail about specific lattice motions is extracted (*20*). Through ISRS, selected lattice modes whose motions are involved in structural change are coherently excited and their responses are observed.

Perovskite ferroelectric crystals and the eight-site model. We have examined the phase transitions in two perovskite crystals, $KNbO_3$ and $BaTiO_3$. A schematic illustration of their crystal structure is shown in Fig. 2A. Because of their fundamental interest as prototype ferroelectrics and their numerous practical applications in nonlinear optics and electrooptics, the structural phase transitions in these materials are among the most extensively studied (*13–19, 21–27*). However, basic qualitative questions about the appropriate microscopic models for the transitions in these and other perovskites have persisted for the reasons described above.

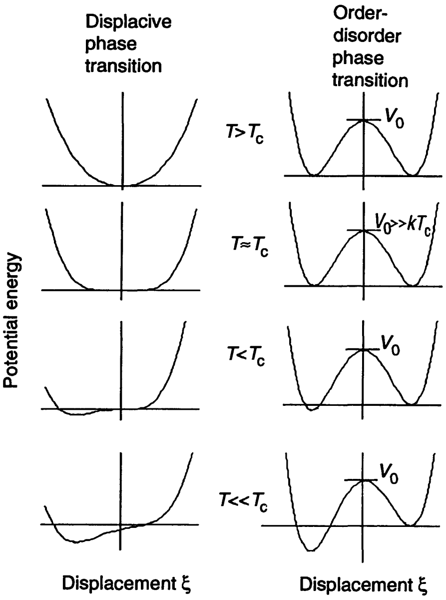

Fig. 1. Local (single unit cell) potential energy diagrams for displacive and order-disorder phase transitions. The displacive transition diagram indicates a single-well potential whose minimum is "displaced" at temperatures below T_c. The curvature of the potential surface is reduced near T_c, corresponding to "softening" of the vibrational mode. The order-disorder transition diagram indicates a multiwell potential surface with a barrier height $V_0 >> kT_c$, where k is Boltzmann's constant. The wells are equal in energy at temperatures above T_c but not below T_c where the lower energy site is favored and ordering occurs. A barrier which is much lower than kT_c or than the zero-point vibrational energy yields displacive behavior.

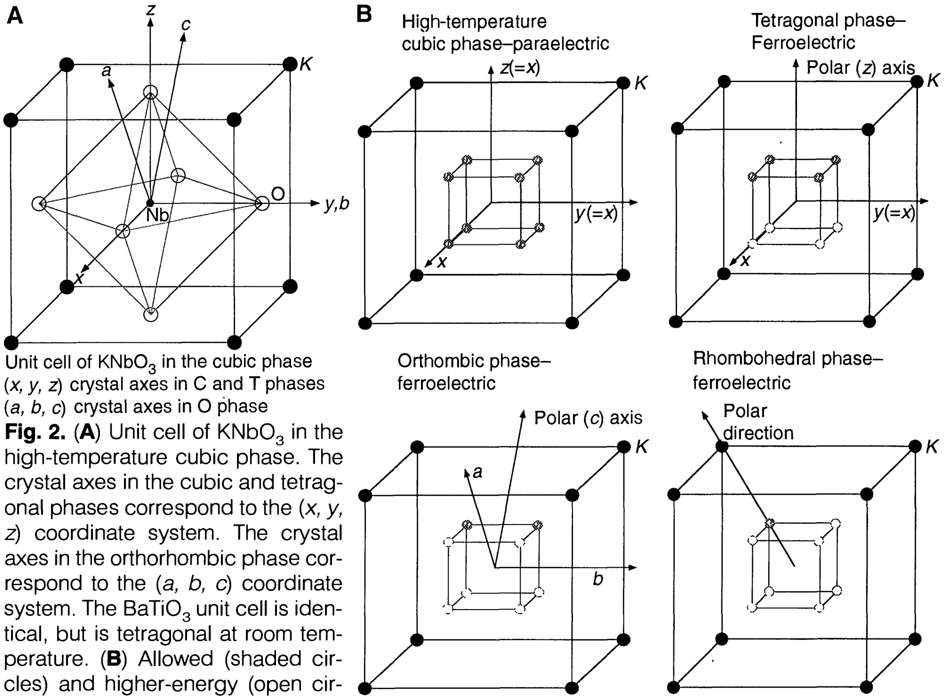

Fig. 2. (**A**) Unit cell of $KNbO_3$ in the high-temperature cubic phase. The crystal axes in the cubic and tetragonal phases correspond to the (*x, y, z*) coordinate system. The crystal axes in the orthorhombic phase correspond to the (*a, b, c*) coordinate system. The $BaTiO_3$ unit cell is identical, but is tetragonal at room temperature. (**B**) Allowed (shaded circles) and higher-energy (open circles) central ion positions in the different phases, within the framework of the eight-site model. In the highest temperature paraelectric phase, the Nb (or Ti) ion may occupy any of eight equivalent sites displaced along the ⟨111⟩ axes toward the corners of the unit cell. The time-averaged position of the ion is at the center of the unit cell. In the tetragonal phase, four sites along a face of the unit cell become energetically favored, with a time-averaged position (and polarization) along the *z*-axis. In the orthorhombic phase, two sites along an edge become favored, and in the lowest temperature rhombohedral phase, one site is favored.

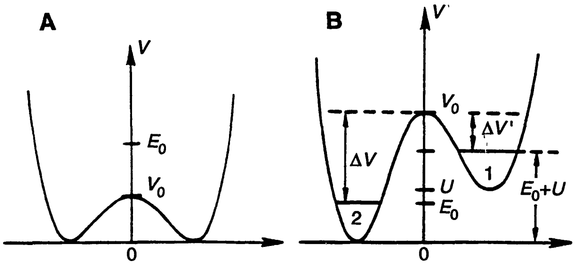

Fig. 3. Projections of the potential energy surface for the central ion along different crystalline directions. (**A**) Between allowed sites, the barrier height V_0 is less than the zero-point vibrational energy E_0. In this case, oscillatory rather than hopping motion occurs. Although distinct potential energy minima are the signature of an order-disorder model, in this low-energy limit the polarization shows displacive behavior. Polarization dynamics along this direction are described by a soft vibrational mode. (**B**) Between allowed and higher energy sites, $V_0 >> E_0$ and thermally assisted hopping motion between minima occurs. The polarization along this direction shows order-disorder character, with dynamics described by a relaxational mode.

With decreasing temperature, the crystals exhibit transitions from a paraelectric cubic phase to tetragonal, orthorhombic, and finally rhombohedral ferroelectric phases. The softening of a transverse optic (TO) phonon mode above each transition temperature (*21, 22*) suggests a displacive model for the transitions. However, symmetry considerations and x-ray (*23*) experimental evidence show that the phase transitions in this crystal family cannot be purely displacive. Much of the available evidence has been interpreted in terms of an "eight-site" model that describes the potential energy surface that dictates the position of the central ion (Nb or Ti) (*23*) (Fig. 2B). In the cubic phase, the time-averaged position of the central ion is in the center of the unit cell, with six oxygen atoms surrounding it along the ⟨100⟩ axes and eight K or Ba ions along the ⟨111⟩ axes at the unit cell corners. The eight-site model proposes that the central ion does not have a potential energy minimum at the center of the unit cell but rather has eight minima along the ⟨111⟩ pseudocubic axes. All eight sites are occupied with equal probability in the cubic phase, but in the tetragonal phase four sites in a plane perpendicular to the ferroelectric axis are preferentially occupied. Two adjacent sites are preferentially occupied in the orthorhombic phase, and one site is preferred in the rhombohedral phase. The eight-site model is also suggested by the vibronic theory of ferroelectricity (*25*) and by computer models of these crystals (*26, 27*).

The eight-site model is an order-disorder model. Ordinarily, only hopping (relaxational) phase transition dynamics can occur in this case. However, if a potential energy barrier between two minima is lower than the zero-point vibrational energy (Fig. 3), then the barrier would exert a negligible influence and motion would be vibrational in character. The eight-site model can account for displacive polarization dynamics in some crystalline directions if it is assumed that the barriers between degenerate allowed sites are low compared to the zero-point energy. Thus motion between allowed sites is vibrational, whereas motion between allowed and higher energy sites occurs through thermally assisted hopping.

Light scattering and dielectric measurements. As in the molecular case, microscopic models of this sort bear on not only the dynamics but also the symmetries and spectroscopic activities of the different modes. We have examined the orthorhombic phase of $KNbO_3$ and the tetragonal phase of $BaTiO_3$, for which the eight-site model predicts Raman-active soft vibrational modes of B_2 and E symmetry, respectively, and relaxational modes of A_1 symmetry. These modes are observable through Raman spectroscopy with different polarization combinations. Because of the heavily damped nature of the soft modes, it has been unclear from B_2 and E symmetry spectra of the two materials whether additional low-frequency relaxational modes with these symmetries, whose central-peak scattering features could easily be masked by those of the soft modes, were also present. Such modes would rule out the eight-site model. Their existence has been suggested not only by the ambiguity of the Raman spectra but, more directly, by in-

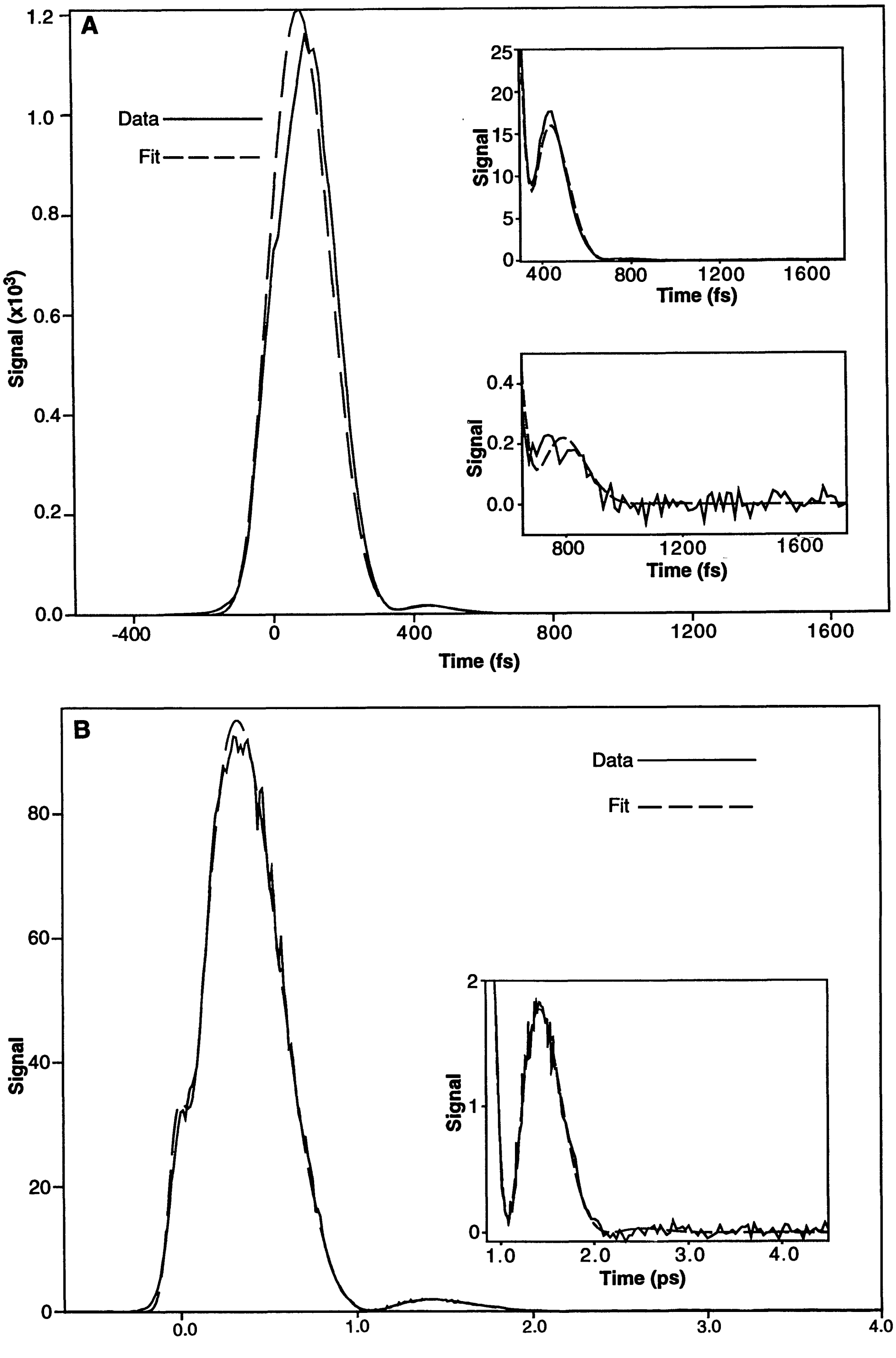

Fig. 4. (**A**) B_2 symmetry ISRS data from $KNbO_3$ at 442.4 K showing the dynamics of the soft phonon-polariton mode. The nuclear response is fit well by a damped oscillator with $\omega = 9.00$ ps^{-1} and $\gamma = 6.14$ ps^{-1}. The scattering angle is 3.97° (in air) and $q = 1.81 \times 10^4$ cm^{-1}. (**B**) E symmetry ISRS data from the soft phonon-polariton mode of $BaTiO_3$ at 321.6 K which is fit as a damped oscillator with $\omega = 2.9$ ps^{-1} and $\gamma = 1.8$ ps^{-1}. The scattering angle is 0.52° (in air) and $q = 2.89 \times 10^3$ cm^{-1}.

consistencies in values of the low-frequency dielectric constant ε_0, which is determined by low-frequency (vibrational and relaxational) polar modes. In each material, there is quantitative disagreement between the value of ε_0 determined through capacitance measurements and the value calculated from the soft mode parameters through the Lyddane-Sachs-Teller (LST) relation. For a crystal with one polar mode, the LST relation is $\varepsilon_0/\varepsilon_\infty = (\omega_{LO}/\omega_{TO})^2$. Here ε_∞ is determined from measurements of the refractive index (and can be modified to include high-frequency lattice contributions), ω_{LO} is the longitudinal polar optic phonon frequency (easily determined from Raman measurements because this mode is not heavily damped), and ω_{TO} is the transverse polar optic phonon (soft mode) frequency (*24*). The disagreement suggests that there exist some polar modes that are not included in the LST calculation [which can be modified to include several modes (*28*)]. It has been assumed that additional low-frequency relaxational modes whose Raman scattering features could easily be obscured by those from the soft mode have gone undetected and could account for the discrepancies. In one Raman study of $KNbO_3$ (*19*), the central scattering feature was interpreted as showing a relaxational as well as a soft vibrational mode of B_2 symmetry. The parameters of both modes together yielded good agreement with the dielectric constant, and based on these results an alternative to the eight-site model was suggested.

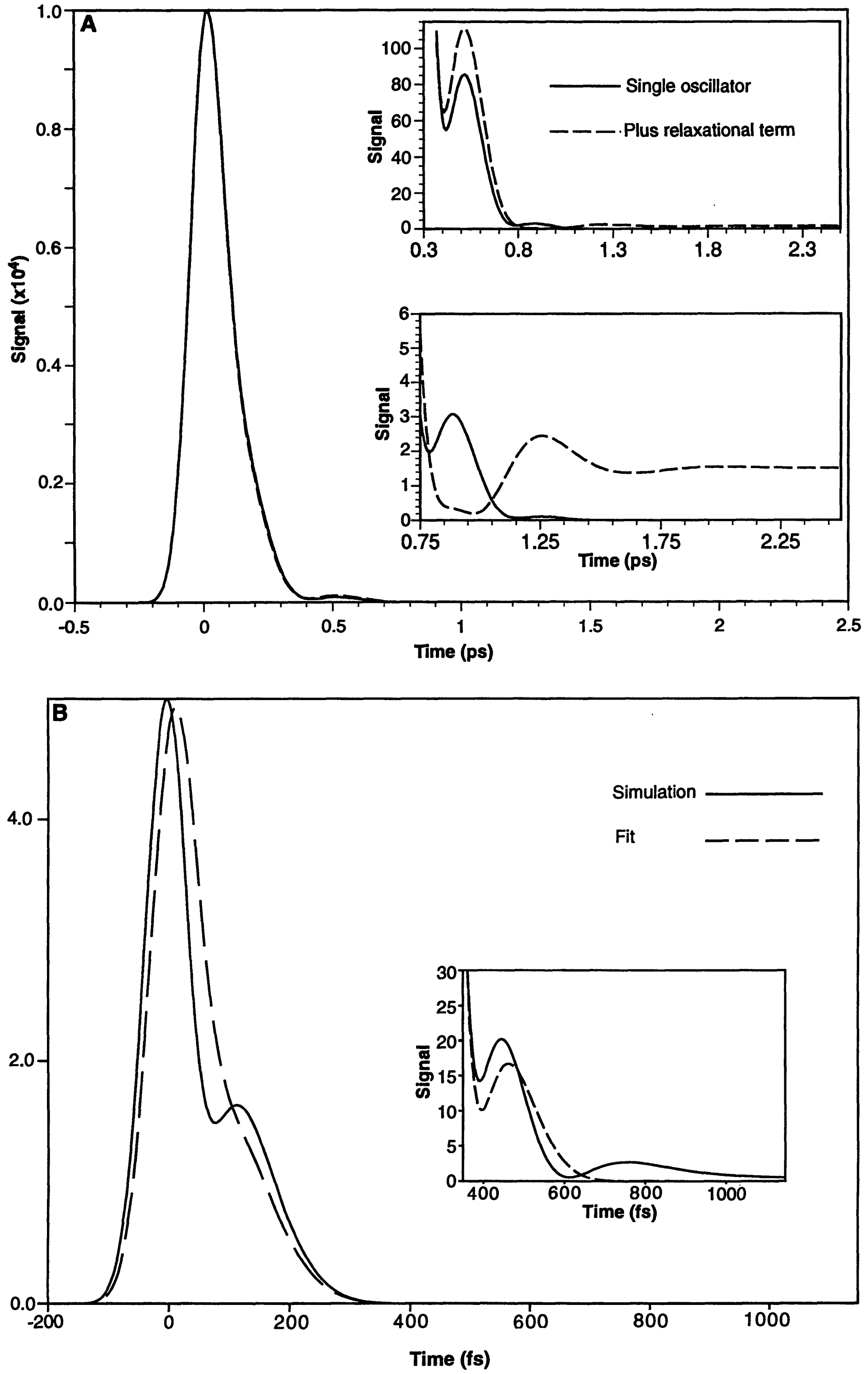

Fig. 5. (**A**) Simulated ISRS data for $KNbO_3$ utilizing a relaxational mode (100-MHz linewidth) with a scattering efficiency of 10^{-4} relative to the soft phonon mode ($\omega = 8.5\ \mathrm{ps}^{-1}$ and $\gamma = 4.5\ \mathrm{ps}^{-1}$). Nonexponential decay of the signal oscillations is apparent. (**B**) Simulated ISRS data (solid curve) based on the results of Fontana *et al.* (*19*) for $KNbO_3$ at 480 K, including a damped oscillator and coupled relaxational mode. Note the highly nonexponential decay of the oscillations. An attempt to fit the simulation with a damped oscillator only is shown to emphasize the difference between this prediction and the results of ISRS experiments.

Femtosecond time-resolved experiments. Our ISRS experiments were conducted in a time-delayed four-wave mixing geometry with 70-fs, 615-nm, 1-μJ excitation and probe pulses (*9*). The selection rules for ISRS are the same as those for conventional Raman scattering. The B_2 symmetry phonon in $KNbO_3$ was excited and probed with an $a + \Delta c$ (bc) $a - \Delta c$ geometry for the pump pulses and for the probe and signal beams. The terms outside and inside the parentheses describe the propagation directions (in the *ac* plane and nearly parallel to the *a* axis) and the polarization directions, respectively. Phonons of *E* symmetry in $BaTiO_3$ were examined with an $x + \Delta y$ (yz) $x - \Delta y$ geometry. The notation has the same meaning as for $KNbO_3$ above except that the (x, y, z) coordinate system refers to the tetragonal axes rather than the (a, b, c) coordinate system of the orthorhombic phase (*21*). Experiments on the relaxational modes were also carried out and will be reported elsewhere (*29*).

The soft modes in $KNbO_3$ were studied at seven temperatures that span the majority of the orthorhombic phase, and the soft modes in $BaTiO_3$ were studied at four temperatures that span the majority of the tetragonal phase. At each temperature, experiments were performed with five scattering angles to probe five different wave vector magnitudes q. The polar modes are dispersive because of phonon-polariton coupling, and observation at several wave vectors is necessary for determination of the uncou-

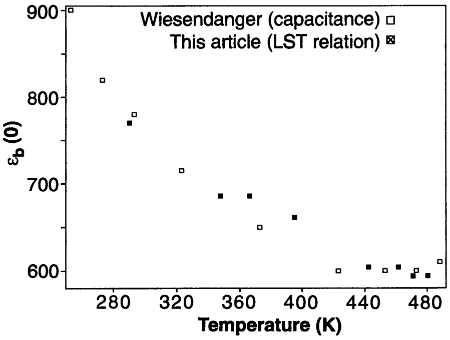

Fig. 6. Low-frequency dielectric constant ε(0) in the orthorhombic phase of $KNbO_3$, determined from ISRS measurements of polariton dispersion and from capacitance measurements (*24*).

pled phonon parameters. This effect has been discussed at length (*30*), and a detailed description of ISRS experiments on dispersive polar modes has been provided (*31*). However, the dispersive properties of the polar modes are of secondary interest here.

Typical data are shown in Fig. 4. Despite the very strong damping of the soft mode, the collective vibrational polarization dynamics are observable in both crystals at all of the temperatures studied. In $KNbO_3$, the soft mode is heavily damped but remains underdamped at all wave vectors and temperatures. In $BaTiO_3$, the soft mode is overdamped at large q but underdamped at small q. The theoretical fits shown with the data were generated by assuming that only a damped oscillator response, that is, $G(t) = A\,e^{-\gamma t}\sin\omega t$, with no relaxational component, occurred. (An instantaneous, purely electronic response that appears only at $t \approx 0$ while the excitation pulses are still in the crystal is also included in the fits.) Our results demonstrate that there are no relaxational contributions along the axes probed. To emphasize the degree to which such contributions can be ruled out, in Fig. 5A we show simulations of ISRS data in which both a heavily damped soft mode with parameters typical of $KNbO_3$ and a relaxational mode of narrow linewidth (100 MHz), with a scattering intensity of only 10^{-4} that of the soft mode, are included. The simulation is based on a response of the form $G(t) = A\,e^{-\gamma t}\sin\omega t + B\,e^{-\lambda t}$ with $(B/A)^2 = 10^{-4}$. [Note that ISRS signal $\propto |G(t)|^2$. The fits and simulations include convolutions for the pulse duration of ~70 fs, as has been discussed in detail (*9*). The fits and convolutions are not highly sensitive to either the duration or temporal shape of the pulses because the features of interest occur on considerably longer time scales.] Even this narrow relaxational contribution, which would be lost under the real and parasitic scattering features in the Raman spectrum, is easily noticed in the ISRS data because it gives rise to highly nonexponential damping of the vibrational signal and to a long-lived signal component that is separable at long times from the soft mode signal. Simulated ISRS data based on the vibrational and relaxational parameters reported in (*19*) are also shown in Fig. 5B, and clearly do not resemble our actual data.

In addition to providing a critical test for the number and character of low-frequency modes, ISRS data permit accurate quantitative characterization of the temperature-dependent soft phonon frequencies and damping rates. These parameters can be used to calculate the low-frequency dielectric constant through the LST relation. The temperature-dependent results from $KNbO_3$ are shown in Fig. 6. The important feature to notice is that quantitative agreement between dielectric constant values determined through capacitance measurements (*24*) and through our measurements is achieved without the need for any relaxational polar modes of B_2 symmetry. Our results taken together offer critical support for the eight-site model in that its qualitative and quantitative predictions for the lattice dynamics and symmetries have been demonstrated.

The ISRS data for $BaTiO_3$ such as that shown in Fig. 4 also clearly rule out any relaxational polar mode of the same symmetry as the soft mode. However, the dielectric constant values determined through capacitance measurements and our results do not yield quantitative agreement as they do for $KNbO_3$. We believe that the phase transition dynamics are described correctly by our results, and we suggest that additional independent measurements of ε_0 need to be conducted.

Femtosecond time-resolved observations of heavily damped soft modes involved in cooperative structural change have been reported. Earlier frequency-domain investigations of these modes yielded conflicting results and, most importantly, left open the possibility that relaxational modes of the same symmetries as the soft modes were present. This possibility, supported by discrepancies between the values of ε_0 determined through capacitance measurements and through Raman spectroscopy of the soft modes, led to fundamental questions concerning the microscopic model of the phase transitions. Our results indicate no relaxational modes of the soft mode symmetries, and thereby support the eight-site model of the phase transitions. For $KNbO_3$, a consistent quantitative description of lattice and dielectric results is provided. Our results demonstrate the value of time-domain methods for detailed examination of heavily damped soft modes near structural phase transitions. The methods should be applicable to many crystalline classes including cooperative Jahn-Teller systems, incommensurate phases, and other types of ferroelectrics.

REFERENCES AND NOTES

1. See for example A. H. Zewail, Ed., *The Chemical Bond: Structure and Dynamics* (Academic Press, New York, 1992).
2. Low-frequency light scattering is described in H. Z. Cummins and A. P. Levanyuk, *Light Scattering Near Phase Transitions* (North-Holland, Amsterdam, 1983).
3. K. A. Muller and H. Thomas, Eds., *Structural Phase Transitions I* (Springer-Verlag, New York, 1981), pp. 1–8.
4. W. Cochran, *Phys. Rev. Lett.* **3**, 412 (1959); *Adv. Phys.* **9**, 387 (1960).
5. P. W. Anderson, in *Fizika Dielektrikov*, G. I. Skanavi, Ed. (Akademii Nauk SSR, Moscow, 1960), p. 290.
6. S. DeSilvestri *et al.*, *Chem. Phys. Lett.* **116**, 146 (1985).
7. Y. X. Yan, E. B. Gamble, K. A. Nelson, *J. Chem. Phys.* **83**, 5391 (1985).
8. Y.-X. Yan and K. A. Nelson, *ibid.* **87**, 6240 (1987); *ibid.*, p. 6257.
9. S. Ruhman, A. G. Joly, K. A. Nelson, *IEEE J. Quant. Electron.* **24**, 460 (1988).
10. S. M. Silence, A. R. Duggal, L. Dhar, K. A. Nelson, *J. Chem. Phys.* **96**, 5448 (1992).
11. L.-T. Cheng and K. A. Nelson, *Phys. Rev. B* **39**, 9437 (1989).
12. K. A. Nelson, in *Raman Spectroscopy: Sixty Years On*, vol. 17B of the *Vibrational Spectra and Structure* series, H. D. Bist, J. R. Durig, J. F. Sullivan, Eds. (Elsevier, New York, 1989), pp. 83–106.
13. J. Etchepare *et al.*, *Phys. Rev. B* **41**, 12362 (1990).
14. Y. Tominaga and T. Nakamura, *Solid State Commun.* **15**, 1193 (1974); *J. Phys. Soc. Jpn.* **39**, 746 (1975).
15. M. DiDomenico, Jr., S. H. Wemple, S. P. S. Porto, R. P. Bauman, *Phys. Rev.* **174**, 522 (1968).
16. G. Burns and F. H. Dacol, *Phys. Rev. B* **18**, 5750 (1978).
17. A. Scalabrin, A. S. Chaves, D. S. Shim, S. P. S. Porto, *Phys. Status Solidi B* **79**, 731 (1977).
18. J. P. Sokoloff, L. L. Chase, D. Rytz, *Phys. Rev. B* **38**, 597 (1988); *ibid.* **40**, 788 (1989).
19. M. D. Fontana, A. Ridah, G. E. Kugel, C. Carabatos-Nedelec, *J. Phys. C* **21**, 5853 (1988); *Phys. Rev. B* **40**, 786 (1989).
20. C. V. Shank, R. Yen, C. Hirlimann, *Phys. Rev. Lett.* **50**, 454 (1983).
21. M. D. Fontana, G. Metrat, J. L. Servoin, F. Gervais, *J. Phys. C* **16**, 483 (1984).
22. Y. Luspin, J. L. Servoin, F. Gervais, *ibid.* **13**, 3761 (1980).
23. R. Comes, M. Lambert, A. Guinier, *Solid State Commun.* **6**, 715 (1968).
24. E. Wiesendanger, *Ferroelectrics* **6**, 263 (1974).
25. I. B. Bersuker and B. G. Vekhter, *ibid.* **19**, 137 (1978).
26. R. E. Cohen and H. Krakauer, *Phys. Rev. B* **42**, 6416 (1990).
27. P. J. Edwardson, *Phys. Rev. Lett.* **63**, 55 (1989).
28. A. S. Barker, Jr., *Phys. Rev.* **145**, 391 (1966).
29. T. P. Dougherty *et al.*, *Phys. Rev. B*, in press. For a preliminary report, see T. P. Dougherty, G. P. Wiederrecht, K. A. Nelson, *Ferroelectrics* **120**, 79 (1991).
30. R. Claus, L. Merten, J. Brandmuller, *Light Scattering by Phonon-Polaritons* (Springer-Verlag, New York, 1975).
31. T. P. Dougherty, G. P. Wiederrecht, K. A. Nelson, *J. Opt. Soc. Am. B*, in press.
32. Supported in part by NSF grant DMR-9002279, NASA grant NAG-1-996, DARPA (Center for Integrated Photonics Technology) grant MDA972-90-C-0037, and by contributions from DuPont and Perkin-Elmer.

12 June 1992; accepted 29 September 1992